IET Research Journals

MICCAI 2018

IET Journals
The Institution of Engineering and Technology

ISSN 1751-8644
doi: 0000000000
www.ietdl.org

Augmenting Microsoft's HoloLens with Vuforia Tracking for Neuronavigation

Taylor Frantz[1,2,*], *Bart Jansen*[1,2], *Johnny Duerinck*[3], *Jef Vandemeulebroucke*[1,2]

[1] *Vrije Universiteit Brussel (VUB), Department of Electronics and Informatics (ETRO), Pleinlaan 2, B-1050 Brussels, Belgium*
[2] *imec, Kapeldreef 75, B-3001 Leuven, Belgium*
[3] *Vrije Universiteit Brussel (VUB), Department of Neurosurgery, Laarbeeklaan 101, 1090 Brussels, Belgium*
* *E-mail: taylor.frantz@vub.be*

Abstract: Major hurdles for Microsoft's HoloLens as a tool in medicine have been access to tracking data, as well as a relatively high localization error of the displayed information; cumulatively resulting in its limited use and minimal quantification. The following work investigates the augmentation of HoloLens with the proprietary image processing SDK Vuforia, allowing integration of data from its front-facing RGB camera to provide more spatially stable holograms for neuronavigational use. Continuous camera tracking was able to maintain hologram registration with a mean perceived drift of 1.41mm, as well as a mean sub two-millimeter surface point localization accuracy of 53%, all while allowing the researcher to walk about a test area. This represents a 68% improvement for the later and a 34% improvement for the former compared with a typical HoloLens deployment used as a control. Both represent a significant improvement on hologram stability given the current state of the art, and to the best of our knowledge are the first example of quantified measurements when augmenting hologram stability using data from the RGB sensor.

1 Introduction

Neurosurgery, a field heavily reliant on medical imaging for preoperative planning and perioperative navigation provides an excellent, though challenging, landscape for the exploration of augmented realty in medicine. Numerous authors have described the disadvantages of current neuronavigation paradigms [1–8]. Of paramount concern is that the attention of the physician is divided between the procedural workspace of the patient and the navigational workspace of the displays on which the data are shown. This requires one to mentally transform and relate the visualized 2D imaging data into 3D physical space, often without the ability to see both at the same time. Augmented reality (AR), using a head mounted device (HMD), addresses both problems by directly rendering 3D models of anatomy, planning information, or other pertinent data into the physician's field of view, aligned with the patient anatomy.

Research into the use of AR for neuronavigation has predominately focused on augmenting information displayed on an external screen, while initial registration and tracking have commonly been addressed using an outside-in approach, i.e. with the aid of external tracking hardware similar to existing commercial navigation systems. This trend is highlighted in the review paper from Guha et al. [1], where a majority of the 33 studies highlighted made use of some form of external tracking, whether for a hand-held camera coupled to an external monitor, or tablet-like device. In contrast, only 4 studies made use of a HMD, and only one of these was capable of self pose estimation. This inside-out approach to tracking eliminates the need for external tracking hardware, reducing OR clutter, avoids line-of-sight problems and could prove to be considerably more cost-effective.

Microsoft's HoloLens, when released in 2016, was one of the first headset devices to implement augmented reality on a commercial scale, and has provided the biomedical field with a unified platform for the development of AR in medicine. Since then, it has been a focus of discussion and research in the context of neuronavigation, as it allows for the potential marriage of the patient with their medical imaging data; a long overdue paradigm shift in the art. It contains an inertial measurement unit, one front facing depth camera and 4 flanking gray-scale cameras used to map the spatial surrounding. Proprietary algorithms perform a fusion of the sensor readings to achieve simultaneous localization and mapping (SLAM), aimed at providing a robust approximation of scene and pose. As such, it is possible to display computer models in the Hololens' optical system, ("holograms" only insofar as Microsoft doublethink), and keep these holograms fixed, up to a certain accuracy, with respect to the physical space as the wearer changes their viewpoint and position.

The spatial alignment of data obtained from preoperative imaging to the patient anatomy is an essential component to any navigation system. The process is typically composed of two steps. During an initial registration step, the correspondence between the patient anatomy and computer model needs to be established. Next, that correspondence needs to be maintained, potentially even after the patient anatomy has moved, which we will refer to as tracking.

Research on the use of the HoloLens for medical interventions has suffered from the lack of access to the raw sensor readings of IR and gray-scale cameras. This has resulted in the use of manual registration methods based on direct visual surface matching in lieu of more traditional automatic IR based schemes, [9, 10]. Furthermore, the perceived spatial stability of any placed hologram can only be as good as the headset localization, and the inability to tune headset tracking for the close range, high accuracy setting of surgery has resulted in tracking errors in neighborhood of $\pm$6mm [11–13].

Registration and tracking using HoloLens' contrived spatial mesh and SLAM system, without access to exact sensor information by Xie et al. [14] indicated that the low vertex density and surface bias of the mesh, as well as uncertainty of the SLAM make this approach unsuitable. Garon et al. [15] went as far as to attach an external depth camera to a HoloLens, thereby bypassing the data limitation. However neither of them reported on accuracy.

The notion of using the HoloLens' RGB camera and image processing techniques for tracking has been suggested as a workaround, as this is an already established technique in machine vision research. Towards the tail-end of papers, the proprietary image processing SDK Vuforia is often highlighted a solution in this regard, as it contains object tracking libraries compatible with HoloLens development [9, 16, 17].

Vuforia's image processing library allows HoloLens to track a known target image from the front facing camera's coordinate system. Therefor the apparent world position of any object whose position is made dependent on that tracked target is then independent of headset localization. Not only does this approach provide

the potential for improved hologram stability, but also for future automatic registration schemes.

Researchers from Duke University appeared to have used Vuforia for the tracking during a simulated external ventricular drain placement, however no results or conclusion have been reported, [18]. The use of RGB data from the front-facing camera in image processing has also been reported on by McDuff et al. [19] and Eckert et al. [20] who applied it towards ballistocardiography and object detection respectively. Yet, to the best of our knowledge, no group has yet published quantitatively the advantages of augmenting HoloLens with object tracking information through the use of Vuforia, or other similar means.

In contrast to the media front by Microsoft concerning Hololens as a tool within the medical field, the current body of published literature concerning its use in medicine is severely under quantified, with many publications (and media demonstrations) being of anecdotal quality. The following text expands on the current body of literature by quantifying the use of Vuforia's SDK in a simulated neuronavigational workflow.

2 Methods

2.1 Segmentation and 3D modeling

Imaging data were provided by physicians from UZ Brussels. Ultimately a 3D printed skull phantom, for which CT data was available, was chosen. Obtained DICOM images were segmented using 3D Slicer to provide masks for bone and neoplastic structures. Segmentation was accomplished by a mixture of thresholding and cut-grow techniques using the plug-in *Fast Cut Grow*. In total three segmentations were made; the skull, and two mass phantoms.

Following segmentation, *3D slicer* was used to construct computer models of each structure. Model geometry was then smoothed using a Laplacian filter over 25 iterations, and then exported in STL format. Due to the rendering hardware limitations of the Hololens, the models were subsampled significantly using the open source program *MeshLab*. Subsampling was accomplished using a quadric edge collapse decimation filter. The complete computer model as well as 3D printed phantom were named Sara, figure 2.

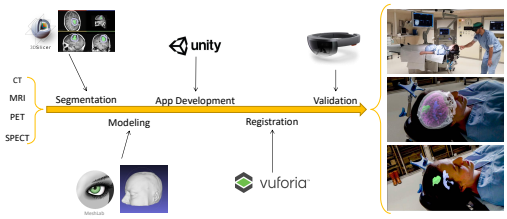

Fig. 1: Overview of the workflow from DICOM to hologram.

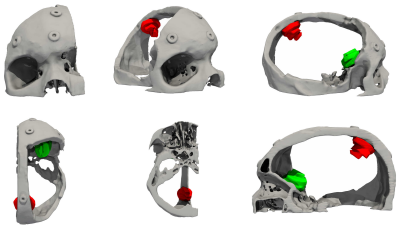

Fig. 2: Sara Model. Top Row corresponds to (left to right) front, isometric and right side view. Bottom row contains (left to right) top, bottom and right side view.

2.2 AR Neuronavigation Application

The personal distribution of the game development engine Unity (version 2017.2.0f3) was used to construct the main application which was to run on HoloLens. The decision to use an outdated Unity build, rather than the current 2018.1 build was due to a known compatibility issues with the latest release (2017) of Microsoft's Mixed Reality Toolkit SDK (MRTK).

All holographic content was placed in a single parent object, whose persistent spatial anchor could be repositioned by the researcher. The models were not given mass or collision boundaries, as this would make it impossible to place them inside a phantom target or person. A single overhead directional light was used in the scene. In addition to this, the detailed phantom models were illuminated with global ambient lighting, ensuring a realistic interventional hardware load. The application was deployed to HoloLens after which it was ensured that performance never fell below 59 FPS.

2.3 Object Tracking

The Vuforia SDK (Version 6.5.22) was used for target tracking. To attenuate fluctuations in Vuforia's tracking output, the positional and rotational averages of 16 frames were taken using a sliding window; no appreciable delay or ill-effect was observed. During tracking, the model's transform was updated as the product of the Camera-Target transform and Target-Phantom transform.

Phantom tracking was accomplished through Vuforia's proprietary feature detection algorithms and a known RGB cylindrical target. Through comparison of extracted visual features on the tracking target and those of the computer model in memory, the 3D rigid transformation of the target can be estimated using a single camera. A priori knowledge of a transform between a well manually registered hologram and the phantom allowed for the consistent automatic manual registration of the hologram to its phantom target when using Vuforia. Continual tracking of the target allowed for this perceived registration to be maintained from any perspective.

Early on, plane image targets were found to be impracticable due to line of sight limitations, and reduced tracking accuracy at high incidence angles between the target and camera. The implementation of a cylindrical target solved this by allowing the target to remain normal to the headset's camera over 360°. To that end, the well performing provided stock Vuforia image *tarmac* was printed onto semi-mat photo paper at 1200 DPI. Measuring 165.7mm in height, and 235.6mm in width, it was then wrapped around a cylinder whose diameter measured 75mm and secured by thin double sided tape in such a manor where it would not be visible, figure 3b.

2.4 Phantom Setup

To measure hologram accuracy, an A4 sheet of millimeter paper whose minor lines were of 2mm spacing, and whose major lines were of 10mm spacing was affixed to a coated expanded polystyrene support board. To this was then affixed via a non-permanent bonding agent the 3D printed Sara skull phantom. This assembly was then secured using common camera mounting hardware to the working end of a tripod. The pitch, yaw, and roll of the tripod's head, and by extension the phantom, was confirmed to be under 1°. The distance between the floor and the XY plane of the millimeter paper was 130cm.

To assure that obtained data were comparable, fixed locations were chosen for repeatability. On the floor, marked points were placed at -90°, -45°, 0°, +45°, and +90° at the distances of 40cm and 80cm from the center of the phantom, figure 3a. These measurement positions were chosen to replicate the distance and range of movement a surgeon may experience during the planning phase of an intervention.

The phantom had been scanned and modeled with a series of radio-opaque fiducials placed at various surface points, figure 2. These were removed from the physical model, however their exact placement was marked on the phantom itself.

IET Research Journals, pp. 1–5

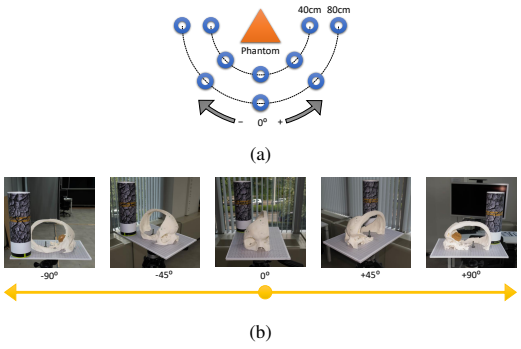

(a)

(b)

Fig. 3: Experimental setup
a Illustration of measurement points relative to the phantom
b View perspectives of the phantom from each angle of measurement

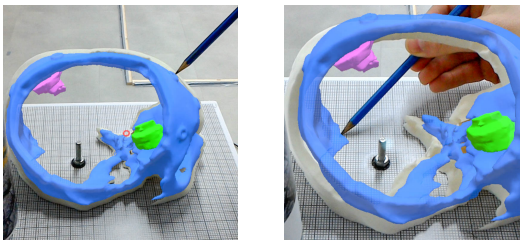

(a) (b)

Fig. 4: Example of measurement techniques.
a Measuring localization accuracy by placing the tip of the stylus into the center of the holographic fiducial.
b Measuring perceived holographic drift by the difference in similar points. Note: The apparent misalignment between the phantom and the hologram seen in both figures is due to the displacement between the RGB camera used to record the scene and the wearers line of sight. From the wearers perspective, the hologram is where it should be.

2.5 Experimental Conditions

Two test conditions were designed to test the efficacy of augmenting HoloLens with Vuforia. The control condition represents a typical device configuration, while the Vuforia test condition included target tracking. As the test lab is static, there was no need to update the spatial map during measurements. A detailed spatial mesh was made of the lab and saved to memory for retrieval.

2.6 Experimental Metrics

Registration time. Quantified by recording the time required by researcher to align the hologram with the phantom using programmed translational and rotational hand gestures. The perceived alignment of surface features was used a the criteria for proper registration.

Hologram drift. Quantified from the perceived translation of the hologram relative to the phantom in the coordinate system of the underlying millimeter paper. Translation in the millimeter paper's Z direction was measured using a ruler. Figure 4b.

Localization accuracy. Quantified by the ability of the researcher to locate a surface point on the phantom based on holographic markers. The center fiducial points of the 3 front markers, still visible on the hologram but not the phantom, are identified by a researcher using a fine tipped stylus. The radial distance from known true center and the perceived center is recorded. Figure 4a.

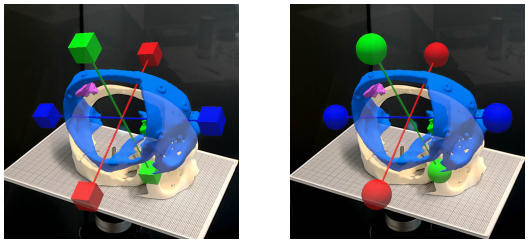

(a) (b)

Fig. 5: Control schemes used for manual transforms of models.
a Translation: Allows the user to axially move the model in either the model or world coordinate system using the "pinch and drag" command.
b Rotation: Allows to user to highlight any axis of the model coordinate system with their gaze and "pinch and drag" to rotate along it.

2.7 Experimental Methodology

Registration was performed once at the beginning of each trial with the researcher standing at 0° and 80cm distance; this was either manual for the control condition, or automatic in Vuforia condition. Only for control trials was registration time noted, as the automatic method was near instantaneous. From this position both perceived hologram translation and surface point localization accuracy were noted. The researcher then moved up to the 40cm distance and repeated the measurements. Following this pattern of 80cm to 40cm distances, data was collected, in order, from the -45°, -90°, $+45^\circ$, and $+90^\circ$ positions. Measurement data obtained from both distances were then aggregated to a single angle.

Multiple iterations of each test condition were performed by an engineering researcher intimately familiar with the program and controls, resetting the program between use. By iterating each test condition it was possible to smooth variance in data, and maintaining a single researcher helped to ensure a consistent bias. This is important as the exact registration of holograms manually is never guaranteed, and translational drift errors rely on the subjective opinion of the researcher. It should be noted that this subjectiveness results from a difficulty to accurately judge matter-hologram boundaries, discussed more in depth later. The decision to reset the program between trial runs was to assure a cold-start, clearing out any data which may have effected future results, and better simulating a clinical use case. Cumulatively data was collected and averaged from 19 trials into the two test conditions.

3 Results

Manual registration times yielded a mean time of 95 seconds, with an minimum and maximum time of 51 and 165 seconds respectively; summarized in table 1.

The mean perceived holographic drift of the control condition was 4.39mm. The Vuforia test condition yielded 68% improved results, with a mean perceived holographic drift of 1.41mm; summarized in table 2. The reduction in perceived drift was statistically significant at all measurement angles, except for 0°, per Student's t-tests at 5% confidence.

The standard error of the mean among all trials for the control condition was 1.29mm. The Vuforia test condition yield 48% more consistent results with a standard error of the mean of 0.67mm.

Surface point localization in the control condition showed a mean error of 5.43mm. The Vuforia test condition yield a 65% reduction, with a mean error or 1.92mm. This resulted in a 34% improvement in sub two-millimeter accuracy vs the control; summarized in table 3. All three points showed a statistically significant improvement vs the control per Welch's t-test at 5% confidence.

4 Discussion

4.1 Registration Time

The obtained data highlights the extreme variability in the ability of the user to register, as best they may, a hologram based on surface features alone. This observation is consistent with the ranges of registration time reported in literature, summarized in Table 1. When comparing the obtained manual registration times to those of Rae et al. [9], when matched like-for-like for an experienced user, our results represent a 45% reduction in mean time, and a 62% and 25% reduction in lower and upper results respectively.

Pratt et al. [10] reported times between one and two minutes per registration, the upper result showing a 27% advantage over our results. It should be noted though, that unlike this study and that of Rae et al., registration was performed on human legs intraoperatively, rather than on head phantoms in a lab.

Cumulatively, registration times from reporting papers in the 2017 Guha et al. [1] review of AR, ranged from 180 to 960 seconds, with a mean of 429 seconds. However, due to the variety in AR implementation and registration techniques between published papers, it would not be appropriate to make direct comparisons between these results and the obtained data. What is clear though is that the use of HoloLens as an AR platform appears to be of great benefit in this metric.

The difference in registration times can be attributed to a number of factors, particularly user experience and control schemes. Dissatisfied by those provided in the MRTK, and taking inspiration from the model controls inside of Unity, iterative collaboration between the engineering team and neurosurgical staff resulted in controls which allowed for precise per-axis model transformation from any perspective; outlined in figure 5.

4.2 Perceived Drift

Table 2 summarizes the difference in mean perceived drift between experimental conditions. The lack of any statistical improvement at 0° is not surprising as the hologram would have been registered either manually or automatically from this position, and the visual effects of holographic drift are often most prevalent while walking *around* a hologram, rather than towards it.

Predominately, the perceived drift when using Vuforia tracking was under 2mm for all angles except for $+90^\circ$, where at 3.42mm it was 278% greater than the mean of other positions. This anomaly was consistent across all trial runs, suggesting that the tracking target may have been compromised in some capacity from that measurement perspective. Despite this, augmenting HoloLens with Vuforia yielded a mean decrease in perceived drift of 68% than without.

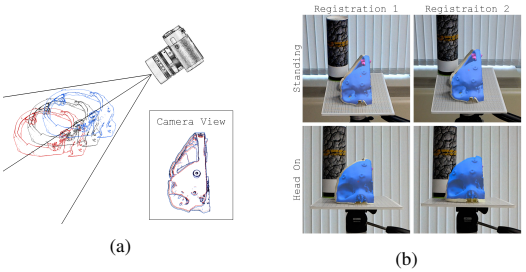

(a) (b)

Fig. 6: Perception of hologram-phantom relationship from a single view
a Similarity of an observed hologram relative to its phantom from a single perspective.
b Two manual registrations highlighting manual registration error. Top row: View from standing; Bottom row: View from head on. Variance in vertical height between each registration may be seen.

Table 1 Comparison of published manual hologram registration times.

Study	Range [s]	Mean [s]
Frantz et al.	51-165	95
Pratt et al.	60-120	NR
Rae et al.	135-219	172

NR: not reported

Table 2 Change in mean perceived drift for each measurement angle.

Condition	$^-90^\circ$	$^-45^\circ$	0°	$^+45^\circ$	$^+90^\circ$	Mean	σ	SEM
Control [mm]	6,27	3,59	0,62	4,60	6,90	4.39	3.34	1.29
Vuforia [mm]	0,83	1,46	1,24	0,08	3,42	1.41	1.08	0.67
Δ	-87%	-59%	0%*	-98%	-50%	-68%	-68%	-48%

* Shown to be insignificant.
σ: Standard deviation.
SEM: Standard error of the mean.

Table 3 Comparison of surface localization results.

Study	<2mm	2-5mm	5-10mm	>10mm
Rae et al.	50%	0%	50%	0%
Frantz et al.				
Matched*	87%	13%	0%	0%
Control	19%	34%	40%	7%
Vuforia	53%	40%	7%	0%

* Results matched to reflect measurements taken from a starting position, without introducing movement.

This reduced standard error of the mean across Vuforia trial runs is most likely due to the consistent transform used for registration. In contrast to this, the less consistent results from the control are most likely due to the difficulty in perceiving exact hologram-matter interactions during manual registration, resulting in poor depth judgment between the two. This is most pronounced when a hologram is registered from a single perspective. Figure 6 highlights this effect.

Auvinet et al. [11] reported deviations in headset localization of $\pm$5.6mm, $\pm$4.4mm, and $\pm$5.2mm along each cardinal direction. Liu et al. [13] reported average headset deviations of 5.6mm, 20.6mm, and 133.8mm for slow, quick, and rapid head movements respectively. Vassallo et al. [12] reported mean hologram localization accuracy of 5.83$\pm$0.51mm while trying to disrupt its tracking through various means. These are all comparable to the perceived drift obtained in the control condition.

4.3 Point Localization

Rae et al. reported on similar metrics used in their experiments, and a comparison can be found in table 3. It is worth noting that due to known holographic drift, their group measured results from only a single position after performing manual registration of the hologram. In consideration of this, we have included a selection of matched results which were taken following registration from the 0° position. It can be seen that before introducing movement associated holographic drift errors, there is a marked improvement vs literature.

This trend continued when analyzing all collected data. Implementing Vuforia tracking yielded similar or better results accuracy across all threshold categories when compared to published literature, while still allowing unabated movements within the test parameters.

4.4 Remarks

One of the challenges when using the active RGB camera tracking was the absolute need to maintain a line of sight between the target and the phantom. This, while not prohibitively difficult at greater distances from the phantom did become so at arm length distance,

where the target, though within visual line of sight, was outside the frustum of the camera. This may be remedied by better placement of the tracking target, use of multiple targets at various key points, and/or rethinking its form. For example, using the RGB camera to track 3D printed objects rather than RGB targets, a feature Vuforia already supports. As for the practicality of such a large marker, Vuforia, or alternative image processing algorithm(s), may effectively be used to maintain an established registration through a secondary reference, the initial registration possibly obtained through the tracking of a smaller stylus and surface matching. This is indeed how workflows are often structured in commercial markerless neuronavigation systems, however unlike these bulkier systems, HoloLens could easily be deployed beyond the walls of an OR.

Limiting manual registration to a single perspective was arguably to the detriment of accuracy in the control, however it does highlight the necessity to adopt automatic registration into AR platforms. This is particularly true in situations where the wearer hasn't the space nor time to manually adapt the registration from numerous perspectives, especially if the registration from one perspective is disturbed due to the tracking inaccuracies of the headset as he/she changes perspectives.

In the scope of medicine, the authors feel that the use of any spatial mapping information is superfluous, as its principal role is to allow holograms to interact with the environment; an unnecessary criteria when one wants to place a hologram inside a head rather than on top of it. A decision to not load, generate, or update any spatial meshing data may therefor further free up already limited hardware resources for future visualization, tracking, or registration tasks.

With the recent release of Microsoft's beta *Redstone* firmware update for HoloLens, the prospect of using data collected from the front facing depth camera becomes reality. Not only does this camera have a greater FOV than the RGB camera, 120° vs 48°, but it also allows for tracking of more familiar, and already in place, instruments in the OR through IR reflectivity.

Having been released in 2016, HoloLens has begun to look outdated vs the competition. Over the last few years the AR industry has not stood idly by, and recent HMD releases from ODG, Meta, and Magic Leap represent significant improvements over HoloLens. Of particular interest are those systems whose optics promise greater depth perception. Still, it is expected that Microsoft will release the replacement for HoloLens, codenamed *Sydney*, sometime in 2019, the delivery of which will keep the workflow and technologies used through this paper relevant for years to come.

5 Conclusion

It was demonstrated that by augmenting HoloLens with Vuforia's RGB target recognition for inside out tracking, significantly greater hologram stability could be achieved than without; thus alleviating one of the greatest hurdles for HoloLens as a tool in neuronavigation. Furthermore, the greater variance between trials obtained when performing registration manually, even by those experienced with HoloLens, highlights the need for more effort placed into automatic workflows, and a reexamination of current practices among many professionals.

6 References

1 Daipayan Guha, Naif M. Alotaibi, Nhu Nguyen, Shaurya Gupta, Christopher McFaul, and Victor X.D. Yang. Augmented Reality in Neurosurgery: A Review of Current Concepts and Emerging Applications. *Canadian Journal of Neurological Sciences*, 44(3):235–245, 2017. ISSN 03171671. doi: 10.1017/cjn.2016.443.

2 Antonio Meola, Fabrizio Cutolo, Marina Carbone, Federico Cagnazzo, Mauro Ferrari, and Vincenzo Ferrari. Augmented reality in neurosurgery: a systematic review. *Neurosurgical Review*, 40(4):537–548, 10 2017. ISSN 0344-5607. doi: 10.1007/s10143-016-0732-9. URL http://link.springer.com/10.1007/s10143-016-0732-9.

3 D Inoue, B Cho, M Mori, Y Kikkawa, T Amano, A Nakamizo, K Yoshimoto, M Mizoguchi, M Tomikawa, J Hong, M Hashizume, and T Sasaki. Preliminary study on the clinical application of augmented reality neuronavigation. *J Neurol Surg A Cent Eur Neurosurg*, 74(2):71–76, 2013. ISSN 2193-6323. doi: 10.1055/s-0032-1333415. URL https://www.thieme-connect.de/products/ejournals/pdf/10.1055/s-0032-1333415.pdf.

4 Fabrizio Cutolo, Antonio Meola, Marina Carbone, Sara Sinceri, Federico Cagnazzo, Ennio Denaro, Nicola Esposito, Mauro Ferrari, and Vincenzo Ferrari. A new head-mounted display-based augmented reality system in neurosurgical oncology: a study on phantom. *Computer Assisted Surgery*, 2017. ISSN 24699322. doi: 10.1080/24699322.2017.1358400.

5 Justin R. Mascitelli, Leslie Schlachter, Alexander G. Chartrain, Holly Oemke, Jeffrey Gilligan, Anthony B. Costa, Raj K. Shrivastava, and Joshua B. Bederson. Navigation-Linked Heads-Up Display in Intracranial Surgery: Early Experience. *Operative Neurosurgery*, 2017. ISSN 2332-4252. doi: 10.1093/ons/opx205. URL http://academic.oup.com/ons/article/doi/10.1093/ons/opx205/4430338/NavigationLinked-HeadsUp-Display-in-Intracranial.

6 Oren M. Tepper, Hayeem L. Rudy, Aaron Lefkowitz, Katie A. Weimer, Shelby M. Marks, Carrie S. Stern, and Evan S. Garfein. Mixed reality with hololens: Where virtual reality meets augmented reality in the operating room. *Plastic and Reconstructive Surgery*, 140(5):1066–1070, 2017. ISSN 00321052. doi: 10.1097/PRS.0000000000003802.

7 Pauline Chauvet, Toby Collins, Clement Debize, Lorraine Novais-Gameiro, Bruno Pereira, Adrien Bartoli, Michel Canis, and Nicolas Bourdel. Augmented reality in a tumor resection model. *Surgical Endoscopy and Other Interventional Techniques*, 32(3):1192–1201, 2018. ISSN 14322218. doi: 10.1007/s00464-017-5791-7.

8 Daniel A Orringer, Alexandra Golby, and Ferenc Jolesz. Neuronavigation in the surgical management of brain tumors: current and Future Trends. *Expert Rev Med Devices*, 9(5):491–500, 2012. doi: 10.1586/erd.12.42.Neuronavigation.

9 Emily Rae, Andras Lasso, Matthew S Holden, Ron Levy, Emily Rae, Andras Lasso, Matthew S Holden, Evelyn Morin, and Ron Levy. Neurosurgical burr hole placement using the Microsoft HoloLens. (March), 2018. doi: 10.1117/12.2293680.

10 Philip Pratt, Matthew Ives, Graham Lawton, Jonathan Simmons, Nasko Radev, Liana Spyropoulou, and Dimitri Amiras. Through the HoloLens looking glass: augmented reality for extremity reconstruction surgery using 3D vascular models with perforating vessels. *European Radiology Experimental*, 2(1):2, 2018. ISSN 2509-9280. doi: 10.1186/s41747-017-0033-2. URL https://eurradiolexp.springeropen.com/articles/10.1186/s41747-017-0033-2.

11 Edouard Auvinet, Brook Galna, Arash Aframian, and Justin Cobb. O100: Validation of the precision of the Microsoft HoloLens augmented reality headset head and hand motion measurement. *Gait & Posture*, 57:175–176, 2017. ISSN 09666362. doi: 10.1016/j.gaitpost.2017.06.353. URL http://linkinghub.elsevier.com/retrieve/pii/S0966636217305763.

12 Reid Vassallo, Adam Rankin, Elvis C. S. Chen, and Terry M. Peters. Hologram stability evaluation for Microsoft HoloLens. 10136:1013614, 2017. ISSN 16057422. doi: 10.1117/12.2255831. URL http://proceedings.spiedigitallibrary.org/proceeding.aspx?doi=10.1117/12.2255831.

13 Yang Liu, Haiwei Dong, Longyu Zhang, and Abdulmotaleb El Saddik. Technical Evaluation of HoloLens for Multimedia : A First Look. *IEEE Multimedia*, pages 1–7, 2018.

14 Tian Xie, Mohammad M. Islam, Alan B. Lumsden, and Ioannis A. Kakadiaris. Holographic iRay: Exploring Augmentation for Medical Applications. *Adjunct Proceedings of the 2017 IEEE International Symposium on Mixed and Augmented Reality, ISMAR-Adjunct 2017*, pages 220–222, 2017. doi: 10.1109/ISMAR-Adjunct.2017.73.

15 Mathieu Garon, Pierre-Olivier Boulet, Jean-Philippe Doiron, Luc Beaulieu, and Jean-FranÂğois Lalonde. Real - time High Resolution 3D Data on the HoloLens. doi: 10.1109/ISMAR-Adjunct.2016.0073.

16 Timur Kuzhagaliyev, Neil T. Clancy, Mirek Janatka, Kevin Tchaka, Francisco Vasconcelos, Matthew J. Clarkson, Kurinchi Gurusamy, David J. Hawkes, Brian Davidson, and Danail Stoyanov. Augmented Reality needle ablation guidance tool for Irreversible Electroporation in the pancreas. 2018. doi: 10.1117/12.2293671. URL http://arxiv.org/abs/1802.03274.

17 Peter Graham. Scopis Announces Holographic Navigation Platform Using HoloLens For Open And Minimally-Invasive Spine Surgery, 2017. URL https://www.vrfocus.com/2017/05/scopis-announces-holographic-navigation-platform-using-hololens-for-open-and-minimally-invasive-spine-surgery/.

18 Kara Manke. Brain surgery may get a bit easier, with augmented reality, 2016. URL https://today.duke.edu/2016/10/brain-surgery-may-get-bit-easier-augmented-reality.

19 Daniel McDuff, Christophe Hurter, and Mar Gonzalez-Franco. Pulse and vital sign measurement in mixed reality using a HoloLens. *Proceedings of the 23rd ACM Symposium on Virtual Reality Software and Technology - VRST '17*, pages 1–9, 2017. doi: 10.1145/3139131.3139134. URL http://dl.acm.org/citation.cfm?doid=3139131.3139134.

20 Martin Eckert, Matthias Blex, Christoph M Friedrich, and Martin Eckert. Object detection featuring 3D audio localization for Microsoft HoloLens. 5(January): 555–561, 2018. doi: 10.5220/0006655605550561.